

In-situ Kinetics Studies on Hydrogenation of Transition Metal (=Ti, Fe) Doped Mg Films

Zhuopeng Tan^{1,2}, Edwin J. Heilweil³, Leonid A. Bendersky¹

¹. Materials Science and Engineering Laboratory, National Institute of Standards and Technology, Gaithersburg, MD, 20899, USA

². Department of Materials Science and Engineering, University of Maryland, College Park, MD, 20742, USA

³ Physics Laboratory, National Institute of Standards and Technology, Gaithersburg, MD, 20899, USA

ABSTRACT

In this paper we report on kinetics studies of the growth rates of a hydride phase during the metal-hydride phase transformation of Mg films doped with transition metals (=Ti, Fe). Infrared emission imaging of wedge-shaped thin films during hydrogen loading reveals different effects of Ti and Fe additives on Mg hydride growth rates. Compared to hydrogenation of pure Mg, Ti addition (atomic fraction 1.6 % and 2.3 %) does not increase the Mg hydride growth rate. However, this doping results in the formation of a thicker hydride layer residing on top of the films. The hydrogenation rate is increased by an order of magnitude for addition of atomic fraction 3.1 % of Fe and the thickness of Mg hydride layer is more than twice that of the hydride layer during hydrogenation of pure Mg. Results obtained here can be used to guide powder design for hydrogen storage applications.

INTRODUCTION

Development of hydrogen storage materials with fast absorption/desorption cycling is essential for advancing a zero emission hydrogen fuel-based economy, especially for the transportation sector [1, 2, 3]. One of the main challenges faced by the development of hydrogen storage materials is the capability of storing hydrogen safely and efficiently. Magnesium hydride, MgH₂, has attracted extensive attention because it is inexpensive, satisfies most safety requirements, has high gravimetric hydrogen capacity (mass fraction 7.6 %), high volumetric density, and good cyclability [4]. However, it suffers from high hydrogen desorption temperature (~552 K) and slow kinetics for on-board hydrogen storage applications under ambient conditions [5].

The influence of transition metals Ti, V, Mn, Fe, Ni, Cu, Zn, Zr etc. on the hydrogenation properties of Mg has been studied extensively [6, 7, 8, 9, 10, 11, 12]. Milanese et al. reported that among nine metals (Al, Cu, Fe, Mn, Mo, Sn, Ti, Zn and Zr), Cu, Al and Zn actively participated in Mg hydrogenation/dehydrogenation, while Cu was the most effective additive for destabilizing MgH₂ [8]. However, after studying the effects of Ti, Mn, Fe and Ni additives on MgH₂ on its thermal stability and decomposition temperature, Ershova et al. concluded that Ti had the largest influence on destabilizing the MgH₂ phase [12]. Fe was not identified to be a promising additive in either study, but theoretical calculations based on first principles performed by Larsson et al indicate that Fe can be a good catalyst for both hydrogen absorption

and desorption [13]. In spite of the large effort made in the past decade to study the effects of transition metal additives on hydrogen storage, many questions remain unanswered, and experimental results are conflicting. In this paper we present experimental results for the measured kinetics of metal hydrides growth for Mg films doped with transition metal additives.

EXPERIMENTAL DETAILS

Pure Mg, $\text{Mg}_{98.4}\text{Ti}_{1.6}$, $\text{Mg}_{97.7}\text{Ti}_{2.3}$ and $\text{Mg}_{96.9}\text{Fe}_{3.1}$ thin films were vacuum co-deposited from two targets at room temperature on 1 cm-long (0001) Al_2O_3 single crystal substrates using electron beam deposition techniques. All targets have purity higher than 99.9 %. A shadow mask connected to a stepping motor was used during the deposition to generate a thickness gradient from 0 nm to approximately 500 nm for the Mg(Ti) films and 0 nm to 350 nm gradient for the Mg and Mg(Fe) films. All films were capped by a 5 nm-thick Pd layer deposited in the same chamber without breaking vacuum. The Pd capping layer was employed to prevent oxidization and facilitate fast dissociation of hydrogen molecules [14]. Film compositions were verified by energy dispersive spectroscopy (EDS) from three positions and an average value was taken to minimize intrinsic EDS system errors.

The heterogeneous growth process of MgH_2 hydride phase in all thin films was monitored by a high-resolution IR camera (256x256 element InSb array; see details on the IR camera in ref. [15]) in a pressurized stainless-steel chamber. Normalized IR emission images were collected every 6 s (for Mg(Fe)) or 10 s (for Mg and Mg(Ti)). Before hydrogen gas was introduced into the reaction chamber, the samples were equilibrated for 2 h under dynamic vacuum at 373 K in order to stabilize the temperature. Mg(Ti) films were hydrogenated at 373 K and 0.3 MPa hydrogen gas pressure for 1 h. Mg(Fe) films were hydrogenated at 373 K and 0.1 MPa hydrogen gas pressure for 1 h. After 1 h hydrogenation, the samples were cooled to room temperature under hydrogen environment.

The hydrogenated thin film cross-sectional transmission electron microscopy (TEM) samples were prepared by a water-free polishing, dimpling procedure followed by ion milling with a cold stage to prevent hydrogen desorption from the thin films.

RESULTS AND DISCUSSION

Representative IR images at different times of hydrogenation for a pure Mg film are shown in Fig. 1 (a)-(c). Before hydrogenation started the IR image shows that the area covered by the film is dark. During hydrogenation, the thinnest part of the film changes from dark to bright and the bright area progresses toward the thicker part of the film (as shown in the frame captured at 30 s and 800 s) with a boundary between dark and bright regions label as "F" (Fig. 1(b) and (c)). Figure 1(d) is a plot of the approximate hydride growth as a function of time determined from the position of F on the recorded IR images (see ref [15] for details). The IR emission intensity increases rapidly in the first 120 s from right to the left, which indicates the fast growth of hydride layer from the top of the film towards the substrate with a thickness of ~110 nm and 1.6 nm/s average growth rate. The growth rate drops dramatically from 1.6 nm/s to 0.03 nm/s afterwards.

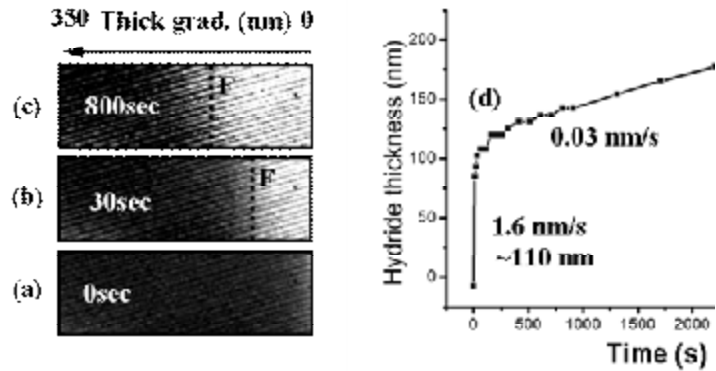


Figure 1. Selected IR images of Mg film hydrogenated for (a) is 0 s, (b) is 30 s and (c) is 800 s. Dashed lines labeled as “F” indicates the approximate boundary position separating the fully hydrogenated bright region from partially hydrogenated dark region. (d) Approximate hydrogenated film thickness as a function of the hydrogenation time.

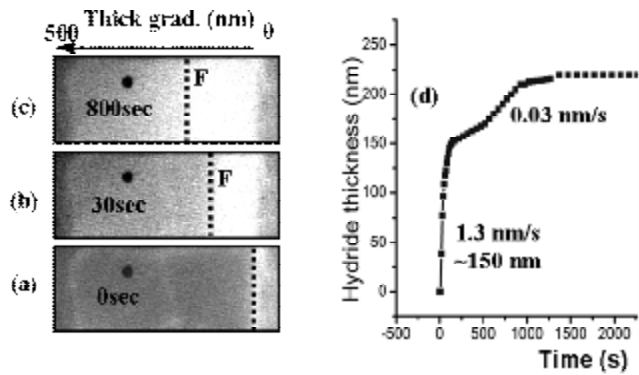


Figure 2. Selected IR images of $Mg_{98.4}Ti_{1.6}$ film hydrogenated for (a) is 0 s, (b) is 30 s and (c) is 800 s. (d) Approximate hydrogenated film thickness as a function of the hydrogenation time.

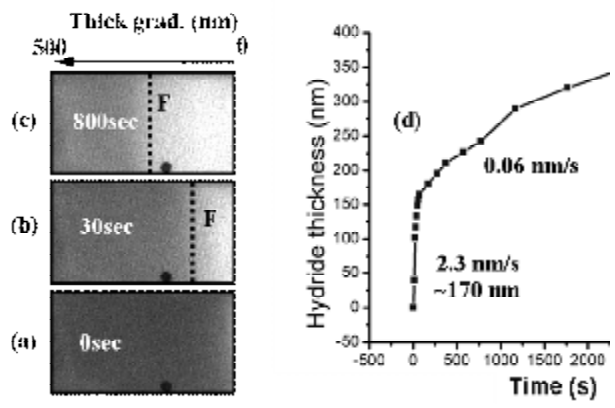


Figure 3. Selected IR images of $Mg_{97.7}Ti_{2.3}$ film hydrogenated for (a) is 0 s, (b) is 30 s and (c) is 800 s. (d) Approximate hydrogenated film thickness as a function of the hydrogenation time.

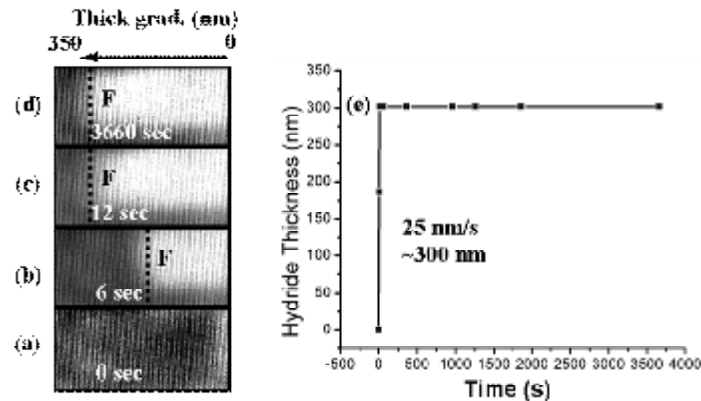


Figure 4. Selected IR images of $\text{Mg}_{96.9}\text{Fe}_{3.1}$ film hydrogenated for (a) is 0 s, (b) is 6 s, (c) is 12 s and (d) is 3660 s. (e) A plot of approximate hydrogenated film thicknesses as a function of the hydrogenation time.

For Mg films doped with Ti of atomic fraction 1.6 and 2.3 %, hydrogenation was carried out at 373 K and 0.3 MPa hydrogen gas pressure. MgH_2 grows also from the top surface towards the substrate with a growth rate of 1.3 nm/s and 2.3 nm/s respectively (Fig. 2 and 3), which are comparable to the pure Mg sample. The hydride layer grew thicker for the Ti doped sample as compared to Mg and the thickness increases with the Ti concentration. The measurements suggest that the films were only partially transformed (top 150 nm of the 500 nm film total thickness), which was later confirmed by TEM measurements.

For Mg films doped with Fe (atomic fraction 3.1 %), hydrogenation was carried out at 373 K and 0.1 MPa hydrogen gas pressure. The reason for the lower gas pressure is to slow down the reaction, which was too fast under 0.3 MPa for the camera to record it. Even for hydrogenation under 0.1 MPa hydrogen gas pressure, MgH_2 grew extremely fast. It only took 6 seconds to move the boundary labeled as “F” more than halfway towards the thickest end (Fig. 4 (a) and (b)). After 12 seconds, the reaction was complete and the emission images remained unchanged (Fig. 4 (c) and (d)). The average MgH_2 growth rate was estimated to be about 25 nm/s (Fig.4 (e)), which is an order of magnitude larger than for the Mg and Mg(Ti) samples. In addition, the hydride layer thickness was found to be about 300 nm, which is close to film’s total thickness. From this result, we conclude that the transformation to the hydride phase for the Fe-doped Mg samples was complete, which was also supported by TEM observations.

These kinetics studies of Mg, Mg(Ti) and Mg(Fe) thickness gradient films allow us to conclude that Ti does not help in improving kinetics of MgH_2 formation, while Fe doping can dramatically increase the hydride reaction rate. These results indicate that to attain the fast and complete hydrogenation of Mg and Mg(Ti) powders [16,17], the powder particle size should be less than 220 nm and 300 nm respectively, with an expected hydrogenation time of about 120 s, while for Mg(Fe) powders, the powder particle size can at least be 600 nm with a reaction time within 12 s. More work is needed to understand the mechanism of the observed catalytic effects of the studied transition metals.

ACKNOWLEDGMENTS

The authors would like to thank Drs. Jason R. Hattrick-Simpers, Chun Chiu, and Wei Zhou for discussions and critical review of the manuscript.

References:

1. DOE. Hydrogen storage, http://www1.eere.energy.gov/hydrogenandfuelcells/storage/current_technology.html.
2. S. Satyapal, J. Petrovic, C. Read, G. Thomas, G. Ordaz. *Catal Today* **120** 246 (2007).
3. G. Principi, F. Agresti, A. Maddalena and S. Lo Russo, *Energy*, **34** 2087 (2009).
4. F. D. Manshester, A. San-Martin, Phase Diagrams of Binary Hydrogen Alloys, ASM International, 83, (2000).
5. J. F. Stampferjk, C. E. Holley and J. F. Scittle, *J. Amer. Chem. Soc.*, **82** 3504 (1960).
6. W. Oelerich, T. Klassen, R. Bormann, *J. Alloys Comp.*, **315** 237 (2001).
7. J. Charbonnier, P. de Rango, D. Fruchart, S. Miraglia, L. Pontonnier, S. Rivoirard, N. Skryabina, P. Vulliet, *J. Alloys Comp.*, **383** 205 (2004).
8. C. Milanese, A. Girella, G. Bruni, V. Berbenni, P. Cofrancesco, A. Marini, M. Villa, P. Matteazzi, *J. Alloys Comp.*, **465** 396 (2008).
9. J. Huot, G. Liang and R. Schulz, *Appl. Phys. A* **72** 187 (2001).
10. J-L. Bobet, B. Chevalier, M.Y. Song, B. Darriet and J. Etourneau, *J. Alloys Comp.*, **336** 292 (2002).
11. S. N. Klyamkin, *Russ. J. Gen. Chem.*, **77** 712 (2007).
12. O. G. Ershova, V. D. Dobrovolsky, Y. M. Solonin, O. Yu. Khyzhun and A. Yu. Koval, *J. Alloys Comp.*, **464** 212 (2008).
13. P. Larsson, C. M. Araujo, J. A. Larsson, P. Jena and R. Ahuja, *PNAS*, **105** 8227 (2008).
14. M. G. Cattania, V. Penka, R. J. Behm, K. Christmann, G. Ertl, *Surf. Sci.*; **126** 382 (1983)
15. H. Oguchi, Z. Tan, E. J. Heilweil and L. A. Bendersky, *Int. J. Hydro. Ener.*, doi:10.1016/j.ijhydene.2009.11.037 (in press) (2009).
16. L. Zaluski, A. Zaluska and J. O. StromOlsen, *J. Alloy. Compd.* **253** 70 (1997).
17. R. A. Varin, T. Czujko and Z. Wronski. *Nanotechnology* **17** 3856 (2006).